Laser and Particle Beams (2011), *29*, 141–152.

doi:10.1017/S0263034611000012

Transient absorption and laser gain in e-beam-excited $Ar/Kr/NF_3(F_2 + N_2)$ gas mixtures

N.N. USTINOVSKII, A.O. LEVCHENKO, AND V.D. ZVORYKIN
Lebedev Physics Institute, Moscow, Russia

(Received 2 November 2010; Accepted 4 January 2011)

Abstract

Newly developed erosion-plasma-source probe technique has been applied for virtually single shot recording of absorption/fluorescence spectra in the 190–510 nm spectral range of e-beam-excited $Ar/Kr/NF_3(F_2 + N_2)$ mixtures. The e-beam excitation rate of about 1 MW/cm^3 is typical of large-volume rare-gas halide lasers. It is experimentally observed that, in Kr/F_2 and Ar/F_2 mixtures, fluorescence and absorption spectra of Rg_2F species are shifted with respect to each other in the opposite direction. Continuous absorption spectrum of Ar_2F excimer is reported, as far as we know, for the first time in the refereed literature. Strong overlapping between the fluorescence and absorption spectra of Ar_2F is responsible for absence of lasing on Ar_2F molecule. Absorption spectrum of Kr_2F excimer is recorded in pure form using the mixture ($Ne/Kr/F_2$) with no alternative broadband absorber. Minor additive of nitrogen to $Ar/Kr/F_2$ mixture or use of NF_3 instead of F_2 has been found to result in broadband optical amplification centered at $\lambda \sim 460$ nm. The maximum optical gain is estimated as about $0.1 \pm 0.05\ m^{-1}$.

Keywords: Gain measurement; Rare-gas halide lasers; Transient absorption probe; UV-visible molecular spectra

1. INTRODUCTION

Interest to studying transient absorption in mixtures of rare gases with fluorine (or fluorine donor) stems from practical importance of e-beam-pumped ultraviolet (UV)-blue excimer lasers on rare-gas halides. One of those, a high-power UV KrF laser with $Ar/Kr/F_2$ gain mixture, has attracted renewed interest as a possible driver for the inertial fusion energy (IFE) (Obenschain *et al.*, 2009). An attractive option seems to be using a broadband Kr_2F transition in the dark blue range (see, e.g., Molchanov (2006) and Huestis *et al.* (1984)) which allows amplification of ultra-short pulses, e.g., second harmonic of femtosecond Ti:sapphire laser, being of interest for the fast-ignition (Basov *et al.*, 1992; Tabak *et al.*, 1994), and shock-ignition (Sherbakov, 1983; Betti *et al.*, 2007) IFE approaches. However, such feasibility is vulnerable to photoabsorption in the gain medium, which affects extraction efficiency from the gain medium (Molchanov, 1988; Zvorykin *et al.*, 2007). Available experimental literature data on transient absorption in rare gas mixtures with fluorine are mainly related to measurements at a few discrete wavelengths, whereas the data on continuous absorption spectra are far from completeness.

In this paper, we examine the origins of transient absorption and effects of adding fluorine and nitrogen to rare gases and their mixtures, as well as using NF_3 as a fluorine donor upon UV-visible absorption and fluorescence spectra under e-beam excitation of up to 1 MW/cm^3 typical of large-scale excimer laser conditions. This laser-oriented study employs our results (Levchenko *et al.*, 2010*a*), in which were recorded the absorption spectra of e-beam excited Ne, Ar, and Kr and their binary mixtures in the 190–510 nm spectral range.

2. EXPERIMENT

Experimental setup and absorption probe technique are described in detail in Levchenko *et al.* (2010*a*, 2010*b*). In brief, the experiments are performed at the preamplifier module of GARPUN laser facility (Zvorykin *et al.*, 2001) using a 1-m-long gas chamber pumped by a 90-ns-long relativistic e-beam with peak current density of about 50 A/cm^2. To improve e-beam-pumping uniformity, a tantalum electron backscattering reflector shaped as cylindrical segment was placed in the chamber about 7 cm behind the foil. Prior to using rare gas-fluorine mixtures, the gas chamber is

Address correspondence and reprint requests to: N.N. Ustinovskii, Lebedev Physics Institute, Leninsky Prospect 53, Moscow 119991, Russia. E-mail: ustin@sci.lebedev.ru

passivated with fluorine-rich mixtures; the gases of high- or very-high-purity grade are used. The absorption spectra are recorded using a charge-coupled device (CCD)-based spectrometer and a pulsed source of broadband probing radiation self-synchronized with e-beam pulse. The same KrF discharge-pumped laser is used both for triggering the e-beam pulse and production of an erosion plasma plume on the target (made of Cu or Teflon) acting as a quasi-point source of 75-ns-long probe radiation. The probe radiation pulse is timed near the maximum of e-beam pumping pulse, with the jitter in timing of ≤ 5 ns.

To obtain a transient absorption spectrum, three data runs (spectra) from the CCD array must be known, namely, the spectra of (1) fluorescence of the e-beam-excited gas under study (probe radiation is "shut off"); (2) "input" probe radiation that passed through the unexcited gas (e-beam gun is switched off); and (3) the mixed signal of the fluorescence from and probe radiation passed through the e-beam-excited gas. The fluorescence spectrum signal is subtracted from the mixed signal, giving the "output" probe radiation signal, and the ratio of the output to input probe signals is a wavelength dependence of the transmittance $T(\lambda)$. In acquiring an absorption spectrum, knowing of the relative spectral sensitivity of the recording apparatus is not necessary since all three data runs are recorded with the same spectral response function whose effect is eliminated completely when data runs are divided by each other. Contrary to the case of pure rare gases, in fluorine-containing mixtures e-beam-induced fluorescence is quite a significant. To record it correctly, the relative spectral sensitivity has been measured using a tungsten band-lamp in the visible 350–510 nm spectral range and a deuterium lamp in the UV range. Small nonlinearity of the CCD array response, observed in the calibrating procedure, is taken into account together with relative spectral sensitivity in mathematical treatment of the acquired data. The measured absorption coefficient is determined as

$$k_{meas}(\lambda) = \ln[1/T(\lambda)]/L \qquad (1)$$

throughout the spectral range under study, where $T(\lambda)$ is recorded transmittance and $L = 112$ cm is the length of the probe beam path in excited gas. It is time-integrated over the probe pulse duration covering the e-beam pulse and its immediate afterglow. Based on accidental variations of absorption spectra (generally one spectrum was measured 3–5 times), we estimate the measurement accuracy as about 15% for absorption coefficients about 1–3 m^{-1}. Small ($\leq$ 0.3 m^{-1}) and high ($\geq$3 m^{-1}) absorption coefficients were measured with worse accuracy.

There are spectral ranges of faulty recording, which are usually hatched in the figures. Those generally appear as absorption valleys related to the line emission in the spectrum of probe radiation and to CCD saturation caused by scattered radiation of the plasma-plume-producing KrF laser and strong fluorescence bands (because of long gas chamber, ArF^* and especially KrF^* amplified spontaneous emission (ASE) at $\lambda \sim 193$ and 248 nm, respectively, can be very intense). Note that use of a diffraction spectrometer for recording a panoramic spectrum in which limiting wavelengths differ more than twice suffers an inherent drawback related to second-order recording: in our case, any spectral feature occurring at wavelength $\lambda \leq 255$ nm is to be replicated in the second order. However, use of an appropriate filter (either a HR 248-nm mirror on quartz substrate or a glass plate) set between the gas chamber and spectrometer to suppress the ASE generally eliminates the problem.

3. RESULTS AND DISCUSSION

Experiments are performed in the following order. Fluorine is first added to pure Ar and Kr, to Ar(He, Ne)/Kr mixtures, and then NF_3 is used instead of F_2. Next, nitrogen is added to $Ar/Kr/F_2$ and to Ar, Kr, and Ar/Kr mixture. The absorption data related to pure rare gases and their binary mixtures presented below in the figures are generally taken from our paper (Levchenko *et al.*, 2010*a*).

3.1. Binary Rare Gas-Fluorine Mixtures

Both fluorescence and absorption spectra of rare gases change with adding fluorine but, in the case of fluorescence, the change is drastic and related to emission of RgF^* and Rg_2F^* (Rg is rare gas symbol) excimers, see, e.g., Huestis *et al.* (1984) and Brau (1984).

Adding fluorine to krypton leads, first of all, to strong well-known KrF (*B-X*) emission at $\lambda \sim 248$ nm. Besides, there arise 275-nm KrF (*C-A*) and broad Kr_2F ($4^2\Gamma \rightarrow 1,2^2\Gamma$) bound-free emission bands (Molchanov, 2006; Zvorykin, 2007; Huestis *et al.*, 1984; Brau, 1984). The fluorescence spectrum shown in Figure 1a was recorded using a 248-nm broadband cut-off filter, which reduced the magnitude of all KrF fluorescences; nevertheless, 248-nm emission reveals itself in the second order. Kr_2F^* emission band has a bell-shaped profile (half-width of about 65 nm) with a maximum at $\lambda \sim 410$–420 nm. Noticeable self-absorption related to Kr I lines is seen at the red wing of the emission profile. The absorption spectrum of Kr/F_2 mixture shown in Figure 1b is seen to be blue-shifted with respect to the spectrum of Kr_2F^* fluorescence and overlapped with it. A blue wing of the recorded fluorescence profile is thus distorted because of volumetric absorption. The fluorescence spectrum has been corrected for volumetric absorption using formula (Shannon *et al.*, 1988)

$$I_{na}(\lambda) = -I_a(\lambda)(\ln[1 - A(\lambda)]/A(\lambda), \qquad (2)$$

where $I_a(\lambda)$ and $A(\lambda)$ are recorded fluorescence and absorption and $I_{na}(\lambda)$ is "true" fluorescence signal that would have been recorded if the absorption had been absent. Corrected fluorescence spectrum $I_{na}(\lambda)$ is shown in Figure 1a; its maximum is just slightly shifted to shorter wavelength compared with the recorded spectrum. The absorption

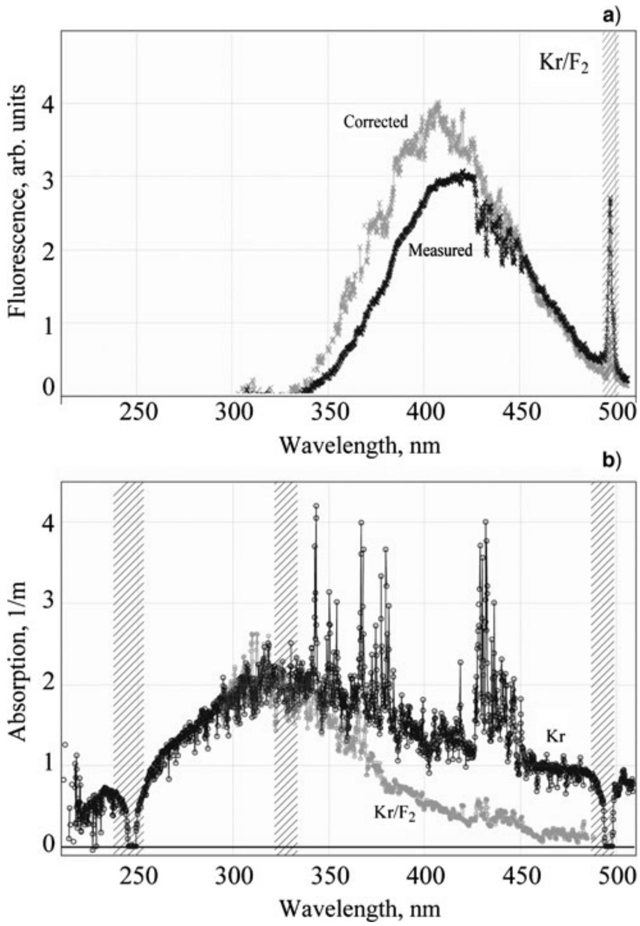

Fig. 1. Spectra of (**a**) fluorescence (recorded with a broadband 248-nm cut-off filter), measured and corrected for volumetric absorption, and (**b**) absorption in $Kr/F_2 = 99.5/0.5$ mixture and in pure Kr at $p = 1.05$ atm.

spectra of Kr/F_2 mixture and pure Kr in Figure 1b are similar in the position of maximum absorption, but different in shape of the long-wavelength tail. Whereas absorbing species in pure Kr is Kr_2^+ (Levchenko *et al.*, 2010*a*), in Kr/F_2 mixture there are also Kr_2F^* triatomic molecules. UV absorption spectrum of the latter related to $(9^2\Gamma \leftarrow 4^2\Gamma)$ transition (as well as all the other spectroscopic properties) was predicted to be very similar to the absorption spectrum of Kr_2^+ (Wadt & Hay, 1978). Experimental study (Geohegan & Eden, 1988) reported the Kr_2F^* absorption profile different from that of Kr_2^+ within spectral range 335–360 nm. However, more recent study (Schloss *et al.*, 1997) based on monitoring the products of photoabsorption showed the absorption profile similar to that of Kr_2^+ predicted in (Wadt, 1980) but more narrow, with half-width of about 33 nm. Similarly, in our measurements, the bandwidth of absorption in Kr/F_2 mixture is smaller than in pure Kr. Line absorption referred to Kr^* (see Levchenko *et al.* (2010*a*)) in Kr/F_2 mixture is certainly lower than in pure Kr. As Kr^* atoms are mainly produced *via* dissociative recombination of Kr_2^+ ions, it is reasonable to assume that UV absorption recorded in the mixture is mainly related to Kr_2F $(9^2\Gamma \leftarrow 4^2\Gamma)$ transition rather than to absorption by Kr_2^+.

Fluorescence spectra of Ar/F_2 mixture at different pressures are shown in Figure 2a. Origin of the fluorescence peaks at 248 nm (497 nm, in the second diffraction order) is caused by traces of Kr in the mixture (KrF (*B*-*X*) transition). ArF^* is responsible for the fluorescence peak at 193 nm (386 nm). The emission continuum centered at $\lambda \sim 275$ nm shows a broad symmetrical profile with a full width at half maximum (FWHM) of about 60 nm; its blue wing recorded in the second order is seen at the long-wavelength part of the spectral range under study. It is assigned, following literature (e.g., Molchanov (2006) and Marowsky *et al.* (1984)) to Ar_2F fluorescence. We have recorded no broadband emission centered at $\lambda \sim 435$ nm observed in (Sauerbrey *et al.*, 1986) high pressure Ar/F_2 mixtures and ascribed to the four-atomic Ar_3F rare-gas halide complex. It is seen in Figure 2a that pressure dependence of the Ar_2F fluorescence intensity is somewhat non-monotonic: it increases with pressure up to $p \sim 1$ atm, and then slowly decreases up to the highest used pressure of 1.8 atm. Non-monotonic dependence of Ar_2F fluorescence

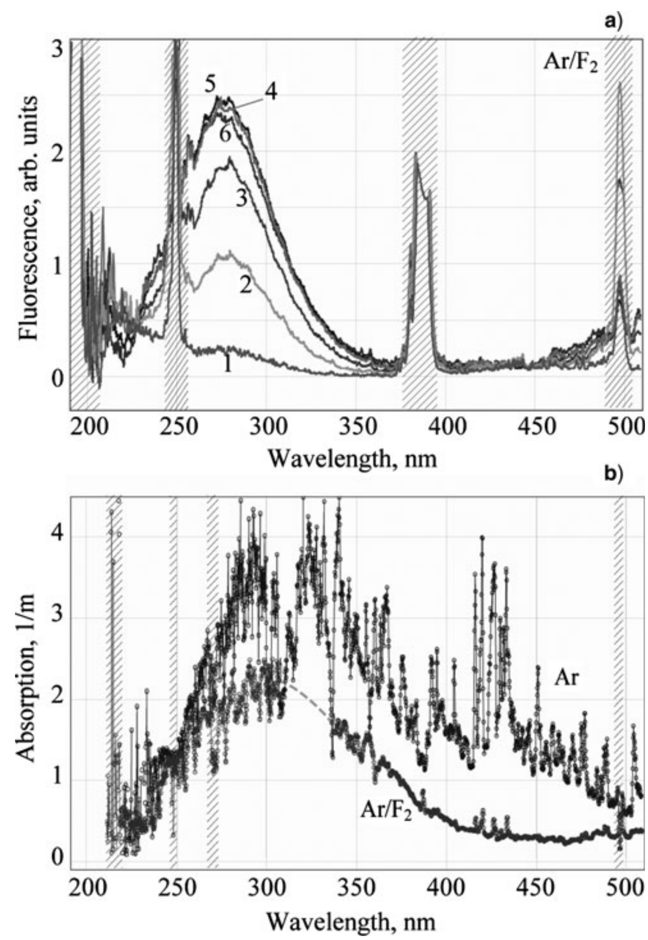

Fig. 2. Spectra of (**a**) fluorescence from $Ar/F_2 = 99.7/0.3$ mixture at $p =$ 0.2 (1), 0.4 (2), 0.6 (3), 0.8 (4), 1.05 (5), and 1.8 (6) atm and (**b**) absorption in Ar/F_2 and pure Ar at $p = 1.8$ atm.

on the mixture total pressure p can be extracted from the literature: one can infer from Figure 6a in Marowsky *et al.* (1982) that maximum of Ar_2F fluorescence in $Ar/F_2 = 99.7/0.3$ mixture occurs at $p \sim 0.7$ atm, at least in the pressure range 0.5–1.1 atm. The pressure dependence of the 193-nm ArF fluorescence (monitored by an independent photodiode) demonstrates monotonic growth with pressure.

Absorption spectrum of Ar/F_2 mixture shown in Figure 2b is a bell-shaped continuum with half-width of about 120 nm and maximum at $\lambda \sim 300$ nm. It was recorded using a Cu target, and the region of faulty recording around $\lambda \sim 327$ nm (see, Levchenko *et al.* (2010*a*)) shown by dashed arc is reconstructed. For the sake of direct comparison, Figure 2b also shows absorption spectrum of pure Ar. To our knowledge, no experimental data on UV absorption continuum in Ar/F_2 mixture have been reported in the refereed literature. Our data are in very good agreement with UV absorption spectra presented in the Los Alamos scientific report (Bigio *et al.*, 1990) and ascribed to Ar_2F and Kr_2F ($9^2\Gamma \leftarrow 4^2\Gamma$) transitions. Like in the case of Kr/F_2, in Ar/F_2 mixture line absorption (by Ar I) and particularly narrow-band absorption corresponding to $Ar_2^*(np\pi\ ^3\Pi_g) \leftarrow Ar_2^*(4s\sigma\ ^3\Sigma_u^+)$ (see Levchenko *et al.* (2010*a*)) transitions are greatly reduced. Consequently, the absorption at $\lambda \sim 325$ nm in the mixture is very unlikely related to photoionization of $Ar_2^*(4s\sigma\ ^3\Sigma_u^+)$. In view of those reasons, we assign the absorption continuum in Figure 2b mainly to Ar_2F. Contrary to the case of Kr/F_2 mixture, the fluorescence spectrum of Ar_2F is somewhat blue-shifted with respect to the absorption spectrum of Ar_2F, which seems strange at first glance. However, such an opposite behavior was predicted in Wadt and Hay (1978) based on the calculated potential curves. In Wadt and Hay (1978), the predicted maximums of the emission from and absorption by Rg_2F ($4^2\Gamma$) state are, respectively, blue- and red-shifted with regard to those shown in Figures 1 and 2, and so in the case of Ar_2F predicted “opposite shift” between the absorption and fluorescence continuums was even larger than that of about 25 nm seen in Figure 2. In the case of Ar/F_2 mixture, because of closeness of the wavelengths corresponding to the absorption and fluorescence peaks, correcting for volumetric absorption (Eq. (2)) leads to no noticeable wavelength shift of the fluorescence maximum but to increase in its magnitude (approximately two-fold at $p = 1.8$ atm). Since absorption increases with pressure, such correcting eliminates above-mentioned non-monotonicity in the pressure dependence of Ar_2F fluorescence. Under the conditions of present experiments, it is the absorption by Ar_2F which seems to be responsible for absence of lasing on Ar_2F molecule rather than absorption by Ar_2^+ and Ar_2^* claimed in Marowsky *et al.* (1982).

3.2. Ternary Ar(He, Ne)/Kr/F_2 Gas Mixtures

Ternary mixtures of rare gases with fluorine (fluorine donor) are common gain mixtures of rare-gas halide lasers (Molchanov, 1988). Fluorescence and absorption spectra of $Ar/Kr/F_2 = 90.7/9/0.3$ mixture, which is a conventional gas mixture of high-power KrF lasers (Zvorykin *et al.*, 2007), are shown in Figure 3. Kr_2F ($4^2\Gamma \rightarrow 1, 2^2\Gamma$) emission band is clearly seen at $p \geq 0.6$ atm. However, at such pressures KrF emission is very strong and must be suppressed with cut-off filter, which makes recording the short-wavelength part of spectrum not possible. The short-wavelength spectrum constituents can be seen at low pressures, when use of the filter is not necessary. One can see in Figure 3a the 220-nm KrF (*D-X*), 248-nm KrF (*B-X*), and 275-nm emission bands. At higher pressures, the 220-nm band is much less intense with respect to the 248-nm band because of strong KrF (*D-B*) collisional quenching. In $Ar/Kr/F_2$ mixture, the 275-nm band is stronger with respect to Kr_2F^* emission than in Kr/F_2 mixture and could be supposed to be a superposition of KrF (*C-A*) and Ar_2F (see Fig. 2a) emission bands. The absorption spectrum of $Ar/Kr/F_2$ mixture is shown in Figure 3b, which also presents absorption spectrum of Ar/Kr mixture. Like in the case of Rg/F_2 mixtures, adding fluorine to Ar/Kr leads to narrowing of absorption profile (~ 90 nm FWHM in $Ar/Kr/F_2$) because of reduction

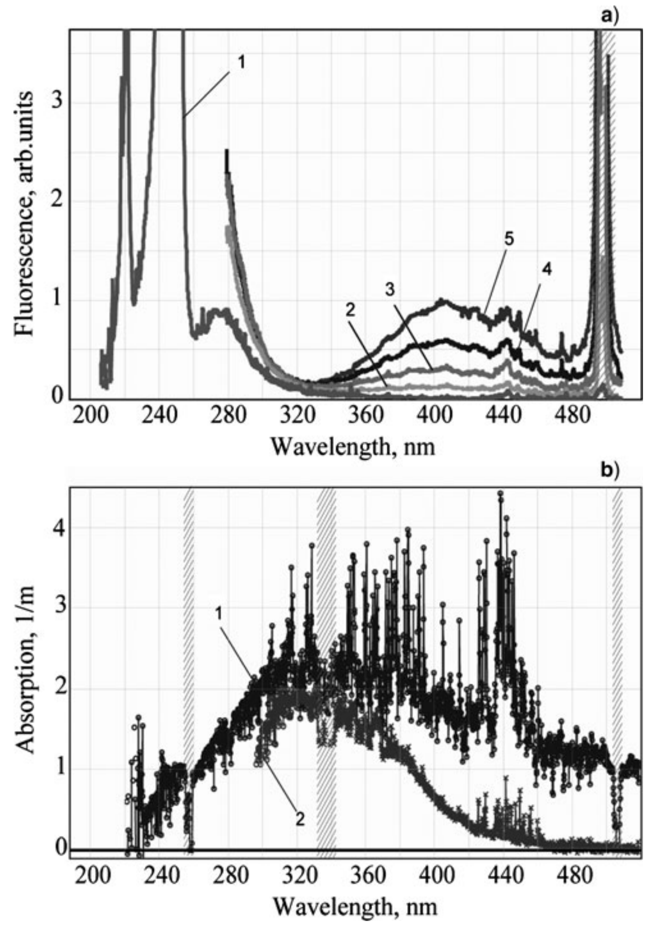

Fig. 3. Spectra of (**a**) fluorescence from $Ar/Kr/F_2 = 90.7/9/0.3$ mixture at $p = 0.2$ (1), 0.4 (2), 0.8 (3), 1.05 (4), and 1.8 (5) atm (at $p > 0.2$ atm, the short-wavelength side is saturated and not shown) and (**b**) absorption in $Ar/Kr = 91/9$ (1) and $Ar/Kr/F_2$ (2) mixtures at $p = 1.8$ atm.

https://doi.org/10.1017/S0263034611000012 Published online by Cambridge University Press

in the long-wavelength part though maximum at $\lambda \sim 310$ nm remains fairly unchanged. Line absorption gets significantly reduced. However, there is no direct evidence that recorded absorption continuum is related completely to Kr_2F^* and in no way to Kr_2^+. If one adds neon instead of argon as a buffer gas to Kr/F_2 mixture, then there will be no absorption caused by Ne_2^+ and Kr_2^+ (Levchenko *et al.*, 2010*a*). Thus, absorption spectrum of $Ne/Kr/F_2$ mixture shown in Figure 4a is completely related to Kr_2F^* absorber (spectrum of Ne/Kr mixture is also shown in Fig. 4a). Nevertheless, it is not possible to evaluate the magnitude of photoabsorption cross-section like it was done in Levchenko *et al.* (2010*a*) for Rg_2^+ absorber in pure rare gas: one has to know both absorber number density and absorption coefficient at some instant. In the case of Kr_2F^* absorber, the difference between the measured integral absorption coefficient $k_{meas}(\lambda)$ (Eq. (1)) and peak absorption coefficient $k_{max}(\lambda)$ corresponding to the instant of maximum absorber number density is expected to be less than in pure rare gases (Levchenko *et al.*, 2010*a*) because of longer lifetime of the absorber. However, to calculate it, as well as the peak absorber number density, one needs to develop a complicated kinetic code, which is not possible because of insufficient knowledge of the reaction rate constants in $Ne/Kr/F_2$ mixture (see, e.g., Section IIIC in Levchenko *et al.* (2010*a*)). In Kr/F_2 and Ar/F_2 mixtures, where kinetics is simpler and more thoroughly studied, recorded absorption continuum may contain contribution from another broadband absorber. Besides, because of strong fluorescence in all the mixtures which is subtracted from the measured signal, accuracy in the present absorption measurements is lower than in Levchenko *et al.* (2010*a*). Comparison of the absorption spectra in Figures 3b and 4a shows that the spectra are fairly similar though that of $Ar/Kr/F_2$ mixture seems to contain little bit of the absorption by Kr_2^+. However, one can consider that dominant absorption in $Ar/Kr/F_2$ mixture is due to Kr_2F ($9^2\Gamma \leftarrow 4^2\Gamma$) transition.

Figure 5 demonstrates virtually linear pressure dependence of the absorption maximum at $p \geq 0.6$ atm. Pressure dependences of the fluorescence at different wavelengths are obtained using appropriate filter set in front of photodiode to select a wavelength of interest. It is seen that pressure dependence of Kr_2F emission is close to quadratic at low pressures, whereas at higher pressures it becomes linear (note that correcting for volumetric absorption hardly changes its slope) and very similar to that of the absorption maximum. Such similarity shows that both fluorescence and absorption maximums are related to the same Kr_2F ($4^2\Gamma$) state. The intensity of KrF (*B-X*) emission band tends to saturate with pressure. The 275-nm emission band shows non-monotonic pressure dependence peaking at $p \sim 0.8$ atm and then significantly decreasing, with specific energy deposition being nearly constant in the pressure range 0.8–1.8 atm (because of backscattering reflector). Adding of Ne to Kr/F_2 mixture leads to great increase in the intensity of 275-nm KrF (*C-A*) fluorescence, with the latter becoming even more intense than 410-nm Kr_2F fluorescence (see Fig. 4b). In $Ne/Kr/F_2$ mixture, pressure dependence of KrF (*C-A*) emission intensity is similar to that of 275-nm band in $Ar/Kr/F_2$ mixture. In both cases, correcting for volumetric absorption

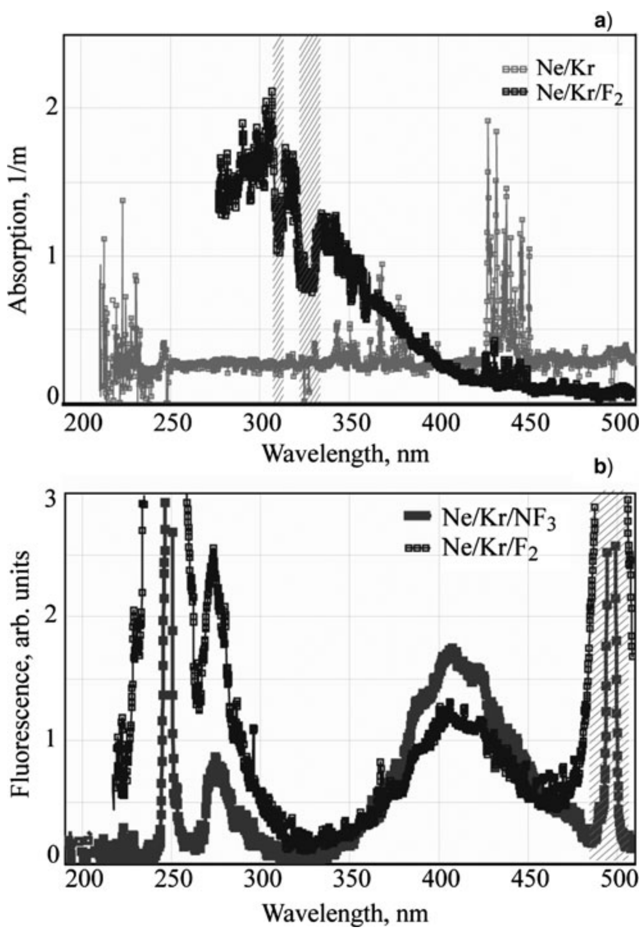

Fig. 4. Spectra of (**a**) absorption in $Ne/Kr = 93.6/6.4$ (1) and $Ne/Kr/F_2 = 93.4/6.4/0.2$ (2) mixtures and (**b**) fluorescence from $Ne/Kr/F_2$ (1) and $Ne/Kr/NF_3$ (2) 93.4/6.4/0.2 mixtures at $p = 2.5$ atm.

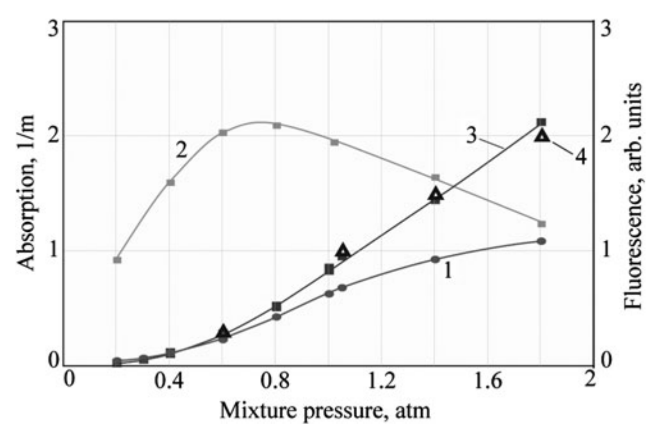

Fig. 5. Absorption at $\lambda \sim 310$ nm (4, triangles) and fluorescence intensity at $\lambda \sim 248$ (1), 275 (2), and 410 nm (3) *vs.* total pressure of $Ar/Kr/F_2 = 90.7/9/0.3$ mixture.

https://doi.org/10.1017/S0263034611000012 Published online by Cambridge University Press

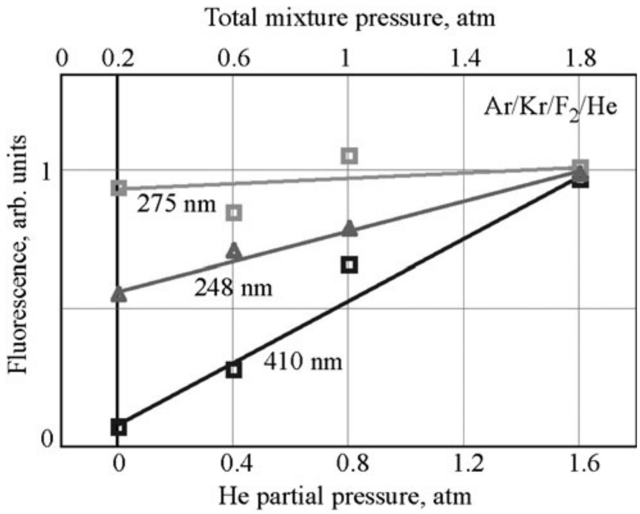

Fig. 6. Fluorescence intensity at $\lambda \sim 248$, 275, and 410 nm, each normalized to its own maximum intensity at $p = 1.8$ atm, *vs*. partial pressure of helium added to $Ar/Kr/F_2 = 90.7/9/0.3$ mixture at $p = 0.2$ atm.

(Eq. (2)) cannot change non-monotonic pressure behavior of the 275-nm fluorescence, unlike the case of Ar_2F fluorescence in Ar/F_2 mixture (see Section 3.1). It is thus likely that in $Ar/Kr/F_2$ (and obviously in $Ne/Kr/F_2$) mixture, the 275-nm fluorescence is related rather to KrF (*C-A*) then to Ar_2F.

In $Ar/Kr/F_2$ mixture, buffer gas Ar, whose main action is to acquire e-beam energy, also participates as a third body in formation of KrF (*via* ion branch) and Kr_2F excimers. Another buffer gas can provide different ratio of the reaction rates for such formation. Figure 6 shows behavior of the emission band intensities in $Ar/Kr/F_2$ mixture at low pressure of 0.2 atm gradually diluted by helium up to the total pressure of 1.8 atm. Taking into account the difference in stopping power of He and Ar, one can see that intensity of the 248-nm emission band increases proportionally to the energy deposition into the $(Ar + He)/Kr/F_2$ mixture. The 275-nm emission (recall that the wavelength matches both Ar_2F and KrF (*C-A*) emission bands) intensity hardly changes with adding He, which can be regarded as an evidence, though indirect, that formation of KrF(C) *via* ion branch with He as a third body is inefficient: otherwise one has to assume, contrary to the above, that Ar_2F emission is mainly responsible for the 275-nm emission band in $Ar/Kr/F_2$ mixture. In contrast, Kr_2F emission intensity (410-nm band) increases greatly with adding helium, in direct proportion to the total pressure of the mixture, whatever the buffer gas.

3.2.1. *Recorded absorption and fluorescence profiles in comparison with literature data*

The Kr_2F $(9^2\Gamma \leftarrow 4^2\Gamma)$ absorption transition is of bound-bound nature. All the six electronic states within the $(4^2\Gamma, 9^2\Gamma)$ segment are strictly bound ($\sim$ 2 eV) with respect to $Kr_2^+ + F^-$ limits, but only $4^2\Gamma$ is stable with respect to the KrF $(D, C, B) + Kr$ limits (Geohegan & Eden, 1988). Hence, the states higher than $4^2\Gamma$ can undergo electronic predissociation provided that there is a relevant crossing repulsive potential curve with either of KrF (D, C, B) + Kr limits. The predissociation seems to occur because (1) absorption on Kr_2F $(9^2\Gamma \leftarrow 4^2\Gamma)$ transition is followed by KrF (*B-X*) emission with quite a high quantum yield (Schloss *et al.*, 1997) and (2) no fluorescence or absorption has ever been observed from the Kr_2F electronic states higher than $4^2\Gamma$. Spectral profile of Kr_2F $(9^2\Gamma \leftarrow 4^2\Gamma)$ absorption band is predetermined by difference potential between the potential curves of the upper and lower electronic states and Franck-Condon overlap integrals, like in the case of emission spectra (Tellinghuisen, 1982). However, a degree of filling of this feasible profile (in other words, particular width of spectrum) depends on relative population of vibrational levels of the absorbing electronic state. Whereas the first two factors are constant, the latter depends on the excitation and quenching conditions. That can be the reason why the recorded bandwidth of Kr_2F $(9^2\Gamma \leftarrow 4^2\Gamma)$ absorption continuum varies from about 33-nm FWHM (optical excitation (Schloss *et al.*, 1997)) to 85-nm FWHM (electric discharge excitation (Greene & McCown, 1989)) and 90-nm FWHM (e-beam excitation, present study). To some extent, the scatter in the measured position of the maximum of Kr_2F $(4^2\Gamma \rightarrow 1,2^2\Gamma)$ bound-free fluorescence varying from about 390 nm (Xu *et al.*, 1993) to 420 nm (Huestis *et al.*, 1984) could also be related to that reason. Another reason can be that the fluorescence spectrum is distorted because of volumetric absorption, with the recorded maximum red-shifted with respect to the true (in the absence of absorption) location (see Section 3.1). The shorter the fluorescence/absorption path the smaller the shift (in Xu *et al.* (1993), the path was as short as about 10 cm). However, correcting for volumetric absorption shifts fluorescence maximum insignificantly even for a fluorescence path of about 1 m (the corrected profile is approximately the same as that shown in Fig. 1a). Note that theoretically predicted Kr_2F fluorescence maximums were at 361 nm $(4^2\Gamma \rightarrow 1^2\Gamma)$ and 371 nm $(4^2\Gamma \rightarrow 2^2\Gamma)$, with much weaker band at 395 nm $(4^2\Gamma \rightarrow 3^2\Gamma)$ (Wadt & Hay, 1978).

3.3. Transformation of Fluorescence and Absorption Spectra of $Ar/Kr/F_2$ Mixture with Adding Nitrogen or Replacing F_2 by NF_3

3.3.1. *Ar(Ne)/Kr/NF_3 Mixtures*

Effect of replacement of F_2 by NF_3 in $Ar/Kr/F_2$ (as well as in $Ne/Kr/F_2$) mixture is illustrated in Figures 4b and 7. As a result, Kr_2F fluorescence intensity ($\lambda \sim 410$ nm) increases, whereas KrF emission decreases significantly, as is shown in Figure 4b by the example of fluorescence spectra of $Ne/Kr/F_2(NF_3)$ mixtures. Both spectra in Figure 4b were recorded under exactly the same conditions. And, as KrF* is commonly believed to be a main direct precursor of Kr_2F^* (see, e.g., Rokni & Jacob, 1982), it seems that 248-nm and 410-nm fluorescences should have changed in unison.

https://doi.org/10.1017/S0263034611000012 Published online by Cambridge University Press

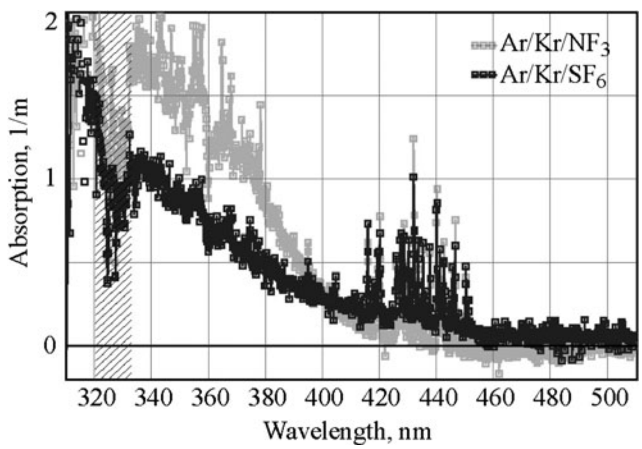

Fig. 7. Absorption spectra of $Ar/Kr/NF_3(SF_6) = 90.7/9/0.3$ mixtures at $p = 1.8$ atm.

Transient absorption within UV range hardly changes with replacing F_2 by NF_3. However, within the blue spectral range of $\lambda \geq 440$ nm it decreases to such an extent that becomes negative (see Fig. 7) indicating an amplification of the probe signal. A negative absorption as high as $-0.05\ m^{-1}$ has been recorded at $\lambda \sim 460$ nm range by optimizing Kr fraction in $Ar/Kr/NF_3$ mixture.

Why do the mixtures with NF_3 and F_2 behave differently? It was believed for a long time that quenching rates of Kr_2F $(4^2\Gamma)$ by F_2 and NF_3 were approximately equal (Huestis *et al.*, 1984). More recent measurements (Xu *et al.*, 1993) show that the former is 14 times larger than the latter; moreover, NF_3 quenches KrF(*B*) 26 times faster than Kr_2F $(4^2\Gamma)$, whereas the rate constants for quenching those species by F_2 differ by only 2.5 times. However, this difference in the quenching rates cannot be an explanation (at least the only one) for increased Kr_2F fluorescence. We used another fluorine donor, SF_6, with the quenching rate constants even more favorable for Kr_2F emission (quenching rates of Kr_2F $(4^2\Gamma)$ by SF_6 and F_2 are as 1 to 250 (Xu *et al.*, 1993), but have not obtained the results comparable with NF_3. Fluorescence intensities of both KrF and Kr_2F in $Ar/Kr/SF_6$ mixture drastically decrease. Both line absorption and UV absorption continuum are lower compared with $Ar/Kr/NF_3$ mixture but the long-wavelength tail of the continuum does not become negative (see Fig. 7). The rate constant for electron attachment to SF_6 (and hence the production rate for F^- ions and the rate of ion channel in formation of KrF) is larger than to F_2. The same was considered to be true for the rate of electron attachment to NF_3 at electron temperatures of 1–2 eV (Chantry, 1982) typical of e-beam-pumped KrF lasers (Brau, 1984). Besides, in contrast to F_2, NF_3 does not absorb KrF 248-nm radiation. Nevertheless, NF_3 (and SF_6 all the more) is less efficient in KrF laser than F_2 (Rokni & Jacob, 1982), despite that ion channel in formation of KrF* is believed to be dominant under e-beam pumping.

In Brau (1984), poor efficiency of NF_3 in KrF laser was explained by decreased rate of neutral channel in production of KrF* since branching ratio towards KrF* in the harpoon reaction of Kr* with NF_3 is less than for F_2 (0.57 against 1.0, respectively). However, the neutral channel is not dominant under e-beam pumping. Another explanation for poor efficiency of NF_3 is ion-molecular charge transfer from Kr^+ to NF_3 reducing the production rate for KrF* and producing positive molecular ions to which electrons may combine (Rokni & Jacob, 1982; Boichenko *et al.*, 2000). Note that following the rate constants commonly accepted at that time (Chantry, 1982; Shaw & Jones, 1977), the rate of such charge transfer was to be much smaller than the rate of electron attachment to NF_3. Later measurements (Miller *et al.*, 1995) that the rate constant for electron attachment to NF_3, (7 ± 4) $10^{-12}\ cm^3/s$ at 300 K, is one and a half orders of magnitude less than that in Chantry (1982) indicate worse efficiency of NF_3 as fluorine donor and support the assumption about relative significance of charge transfer from Kr^+ to NF_3.

3.3.1.1. Discussion on feasible cause for blue radiation alternative to Kr_2F. Chemistry of the reaction between $Kr^+(Kr^*)$ and NF_3 is complicated and gives rise to various species. One can assume existence in the mixtures with NF_3 of another precursor for Kr_2F $(4^2\Gamma)$ alternative to KrF*, which is particularly evident in the case of $Ne/Kr/NF_3$ mixture. Indeed, of all the four possible immediate precursors for Kr_2F^* in $Ar/Kr/F_2$ mixture (KrF*, ArKrF*, Kr_2^+, and Kr_2^* (Boichenko *et al.*, 2000), in order of decreasing importance), only two (KrF* and Kr_2^*) are present in $Ne/Kr/NF_3$ mixture: NeKrF* complex is not known to exist, whereas Kr_2^+ is absent (see Fig. 4a and Levchenko *et al.* (2010*a*)). It is known that NF_3-containing mixtures do not recycle (e.g., in XeF laser), which is related to irreversible decomposition of NF_3 in reaction $2NF_3 \rightarrow N_2 + 3F_2$ resulting in formation of some amount of nitrogen (Mandl & Hyman, 1986). Then, e.g., an N_2KrF^* excimer (formed *via* three-body reaction of KrF(*B*) with nitrogen) can be assumed as one of direct precursors to Kr_2F. In Basov *et al.* (1980) and Zuev *et al.* (1981), N_2KrF^* was supposed to be an intermediate stage in formation of Kr_2F and was reported responsible for emission in the range around $\lambda \sim 450$ nm. It is thus possible that increased fluorescence in the blue region could be related not only to Kr_2F. The features discussed seem to be a reason why a gain medium of Kr_2F laser, which operates at $\lambda \sim 435$ nm (Tittel *et al.*, 1980), is $Ar/Kr/NF_3$ but not $Ar/Kr/F_2$ mixture. In light of above discussion, it is of necessity to study the effect of adding nitrogen to $Ar/Kr/F_2$ mixture.

3.3.2. *$Ar/Kr/F_2/N_2$ Mixture*

Adding nitrogen to $Ar/Kr/F_2$ mixture is found to reduce transient absorption, although unequally throughout the spectral range under study. Within quite a broad interval in the range from 410 to 500 nm, it is reduced to a negative value. Figure 8 shows a part of the absorption spectrum of $Ar/Kr/F_2 = 90.7/9/0.3$ mixture at pressure of 1.7 atm to which 0.08 atm of nitrogen is added. Weak negative

https://doi.org/10.1017/S0263034611000012 Published online by Cambridge University Press

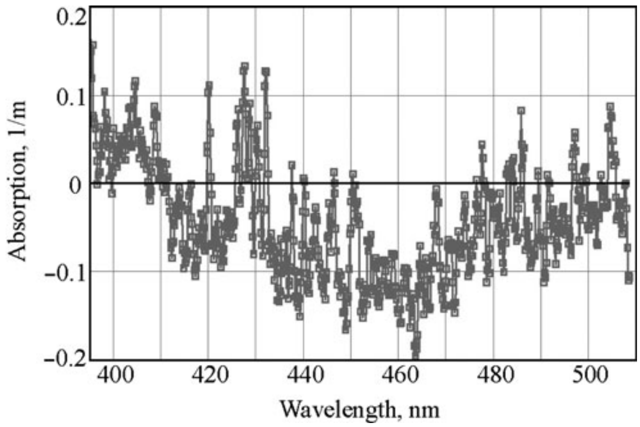

Fig. 8. Part of the absorption spectrum of $Ar/Kr/F_2/N_2$ mixture at $p \approx 1.78$ atm with N_2 partial pressure of 0.08 atm.

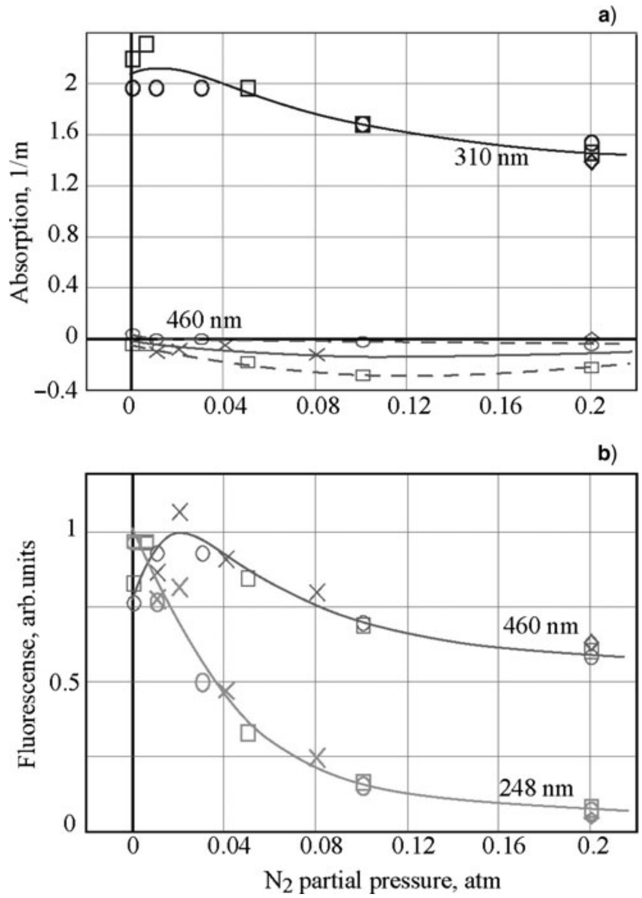

Fig. 9. Absorption (**a**) and fluorescence (**b**) in $Ar/Kr/F_2 = 90.7/9/0.3$ mixture at $p = 1.7$ atm at wavelengths of (a) 310 and 460 nm and (b) 248 and 460 nm *vs*. pressure of nitrogen added to the mixture. Different symbols correspond to different measurement runs.

absorption (in other words, amplification) is seen to occur; there are a lot of absorption lines that "notch" and even break the amplification region, especially at the short-wavelength side. The lines are mainly related to Kr I spectral lines but there are also those related to Kr_2^* and even to Ar I (e.g., 420.1-nm line) (Levchenko *et al.*, 2010*a*). The most broad "amplification band" is centered at about 460 nm being red-shifted with respect to the maximum of Kr_2F ($4^2\Gamma \rightarrow 1{,}2^2\Gamma$) fluorescence band. The result of optimization of the amplification magnitude at $\lambda \sim 460$ nm by varying pressure of N_2 additive is shown in Figure 9a. Nitrogen is added to $Ar/Kr/F_2 = 90.7/9/0.3$ mixture at $p = 1.7$ atm. Particular symbols are related to different measurement runs, which may differ in some experimental features, such as scheme alignment, different optics, etc. Two dashed curves are related to the "most different" data sets. However, all the recorded dependences are "smooth" and show weak amplification in all the measurement runs, so the averaged curve (the solid curve) is expected to reflect the true behavior. The optical gain can be assumed to lie in the range from 0.05 m^{-1} to 0.15 m^{-1}. Evolution of the 310-nm absorption maximum with adding nitrogen is also shown in Figure 9a. Added nitrogen slightly reduces the width of absorption profile in $Ar/Kr/F_2$ mixture because of shortening the long-wavelength tail: small additions of nitrogen reduce the long-wavelength 460-nm absorption but hardly affect the absorption maximum, which might be even somewhat increased. The effect of nitrogen upon fluorescence from $Ar/Kr/F_2$ mixture is illustrated in Figure 9b. Fluorescence intensities at $\lambda \sim 248$ nm (KrF (*B-X*)) and $\lambda \sim 460$ nm behave quite differently. The 460-nm fluorescence shows local maximum for small nitrogen additive, whereas 248-nm fluorescence monotonically drops with increasing nitrogen pressure.

It is seen from above that both replacing F_2 by NF_3 in and adding small amount of nitrogen to $Ar/Kr/F_2$ mixture affect the fluorescence and absorption spectra in a similar manner. However, as further increase in the pressure of nitrogen additive leads for a while to increase in the magnitude of negative absorption, 460-nm fluorescence intensity begins to decrease, and maximum amplification in the blue spectral range is reached when fluorescence has already dropped below initial level. Hence, there has to be another reason for increasing negative absorption in the blue range different from hypothetical amplification by N_2KrF^* or some other nitrogen-containing species. Note also that 410-nm fluorescence related only to Kr_2F ($4^2\Gamma \rightarrow 1{,}2^2\Gamma$) transition behaves with adding nitrogen similarly to 460-nm fluorescence. There are some obvious effects of adding nitrogen to $Ar/Kr/F_2$ mixture related to that nitrogen is efficient vibrational relaxant. First, it is significant decrease in electron temperature in the course of electron-impact vibrational excitation of N_2 molecule, to the value of a few tenths of an eV (Sauerbrey *et al.*, 1982). Since the dependence of the rate constant for electron attachment to F_2 on electron temperature is monotonically declining (Chantry, 1982), there is to occur an increase in the electron attachment rate constant. However, like in the case of replacing F_2 by NF_3, such increase is followed by decrease in KrF^* number density. Apparently, electron attachment to F_2 is a dominant process of electron loss both with and without N_2 additive. Irrelevance of the increased rate of electron attachment for enhanced formation of Kr_2F has also been demonstrated above by the example of SF_6-containing mixtures. Another effect of adding nitrogen is efficient vibrational-vibrational (VV) relaxation of excited molecules, particularly Kr_2F, in the collisions with nitrogen. Both fluorescence and absorption at $\lambda \sim 460$ nm are related to Kr_2F ($4^2\Gamma$) but to different v levels. Taking into account that absorption peak is much farther from 460 nm than fluorescence maximum, it is reasonable to assume that, in the case of absorption, v is higher. Vibrational relaxation will then reduce absorption rather than fluorescence, and the gain can exceed the absorption loss at $\lambda \sim 460$ nm.

3.3.2.1. Comparison with literature data on $Ar/Xe/CCl_4/N_2$ mixture. Somewhat similar situation was observed for e-beam-excited $Ar/Xe/CCl_4$ high-pressure mixture (Sauerbrey *et al.*, 1982) where adding nitrogen led to increase in the output energy of Xe_2Cl laser ($\lambda \sim 515$ nm). Like in our case of $Ar/Kr/F_2$ mixture, the rate constant for electron attachment to CCl_4 halogen donor greatly increased with adding nitrogen though fluorescence of $XeCl^*$ (a precursor to Xe_2Cl^*) decreased. However, the intensity of Xe_2Cl^* fluorescence was relatively insensitive to addition of nitrogen over a broad range of N_2 partial pressure. It was said (Sauerbrey *et al.*, 1982) that production rate of Xe_2Cl^* is not affected by N_2 but modeling showed that number densities of the absorbing species Xe^*, Xe_2^+ and presumably Xe_2^* (the latter is misprinted in Sauerbrey *et al.* (1982)) decrease with nitrogen. This reduced absorption was assumed to be responsible for increasing output of Xe_2Cl laser. Let us note that, in the case of Xe_2Cl^*, self-absorption seems to be insignificant: the absorption and emission profiles related to $Xe_2Cl(4\,^2\Gamma)$ are more separated than those of Kr_2F ($4\,^2\Gamma$). The reason is that Xe_2Cl^* absorption is significantly blue-shifted with respect to Xe_2^+ $1(1/2)_u \rightarrow 2(1/2)g$ UV absorption (McCown *et al.*, 1985), whereas absorption profiles of Rg_2F^* species are similar to those of Rg_2^+ (see, e.g., Section 3.1).

Taking into account complicated kinetics in $Ar/Kr/F_2/N_2$ gas mixture, it seems to be of interest to examine transient absorption in the mixtures of argon and krypton with nitrogen.

3.4. Ar/N_2, Kr/N_2 and $Ar/Kr/N_2$ Mixtures

In the spectral range under study, no measurable fluorescence was observed in e-beam excited Ar, Kr, and Ar/Kr gas mixture (Levchenko *et al.*, 2010*a*). However, even small additive of nitrogen to argon leads to origin of strong well-known fluorescence corresponding to $(0 \rightarrow 0)$, $(0 \rightarrow 1)$, and $(0 \rightarrow 2)$ $v' \rightarrow v''$ transitions of the second positive band system $C^3\Pi_u \rightarrow B^3\Pi_g$ of molecular nitrogen (Pressley, 1971; Ernst *et al.*, 1979) centered at 337.1, 357.7, and 380.5 nm, respectively. In our experiments, the 357.7-nm emission line is much stronger than the others, which disagrees with early observations of the spontaneous emission from e-beam-excited Ar/N_2 mixtures that intensities of 337.1-nm and 357.7-nm emission lines are nearly equal (Ernst *et al.*, 1979). The energy is known to be transferred from metastable Ar atoms to N_2 via resonant reaction

$$Ar^*(4s) + N_2 \rightarrow Ar + N_2^*(C^3\Pi_u, v' = 0). \quad (3)$$

When nitrogen is added to pure Kr or Ar/Kr mixture, no fluorescence is detected (more exactly, it is within the noise level, if any). Indeed, it is known from the literature (Levchenko *et al.*, 2010*a*; Brau, 1984) that, in Ar/Kr mixture with minor additive of Kr, excitation is efficiently transferred from argon (mainly from atomic and molecular ions) to krypton with subsequent production of Kr^* ($5s$). The energy of $Kr^*(5s)$ levels is lower than that of $Ar^*(4s)$ levels, and

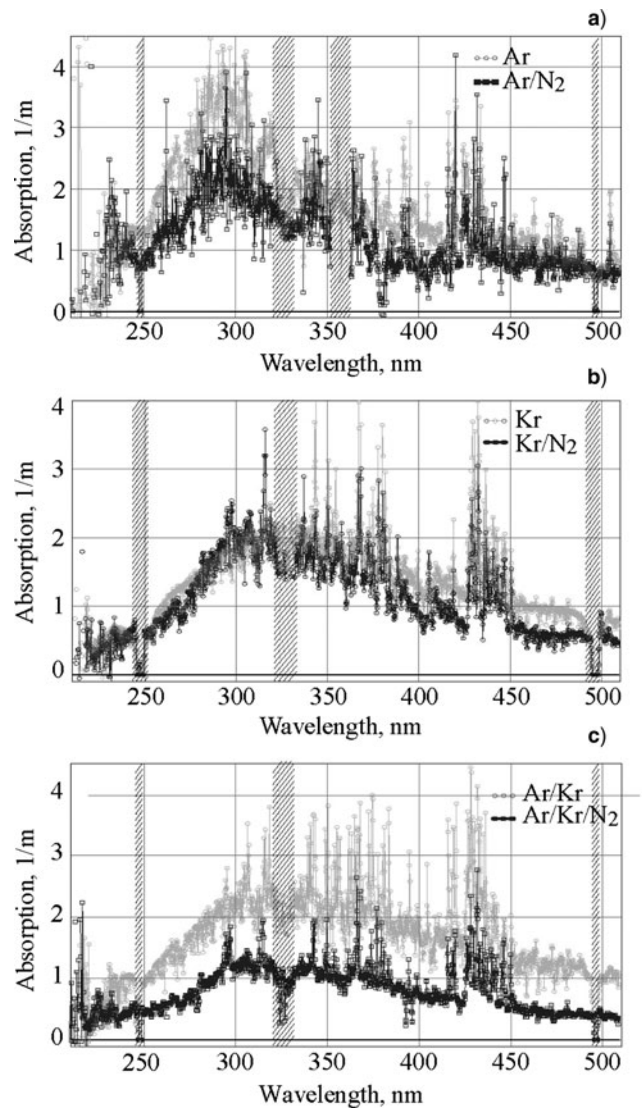

Fig. 10. Absorption spectra in (**a**) pure Ar and $Ar/N_2 = 1.75/0.05$ mixture at $p = 1.8$ atm, (**b**) pure Kr and $Kr/N_2 = 0.95/0.1$ mixture at $p = 1.05$ atm, and (**c**) $Ar/Kr = 1.64/0.16$ and $Ar/Kr/N_2 = 1.6/0.16/0.05$ mixtures at $p = 1.8$ atm.

energy transfer to nitrogen in reaction of type (3) becomes impossible.

Absorption spectra of the mixtures with nitrogen show some interesting features (see Fig. 10). Already small addition of nitrogen (in amount of about 3%) to argon leads to significant decrease in the absorption maximum at 295 nm (related to Ar_2^+ (Levchenko *et al.*, 2010*a*)). That is surprising taking into account that the energy transfer is believed to go *via* reaction (3) and Ar*(4*s*) is produced after dissociative recombination of Ar_2^+. In other words, loss of Ar*(4*s*) is not to affect the number density of higher-energy Ar_2^+. Unfortunately, the spectra have been recorded using a Cu target and thus the absorption peak at 325 nm related to Ar_2^* is not seen in pure Ar (Fig. 10a). Because strong 357.7-nm emission saturates the CCD, absorption around 357.7 nm in Ar/N_2 mixture is not as well represented in Figure 10a. Note that 325-nm peak is to be decreased with nitrogen because reaction (3) reduces number density of the atomic precursor for Ar_2^*. Contrary to the case of argon, even rather significant addition of nitrogen (in amount of about 10%) to krypton does not affect the absorption maximum although somewhat reduces its long-wavelength fraction (Fig. 10b). Similarity (both in the shape and magnitude), between the absorption spectra of pure Kr and Ar/Kr mixture was discussed in detail in (Levchenko *et al.*, 2010*a*): in both cases, absorption is caused by Kr_2^+ ions. It is however seen in Figure 10c that even small (~ 3%) addition of nitrogen to Ar/Kr mixture significantly reduces (approximately halves) the absorption. Further increase in nitrogen number density (up to about 17% of the total pressure) does not significantly affect the absorption. On comparing Figures 10a, 10b, and 10c, one has to assume that, besides well-known reaction (3), nitrogen "captures" excitation from high-lying energy states of argon. We may suggest it occurs *via* reaction (Smith *et al.*, 1980)

$$Ar^{2+}(^3P) + N_2 \rightarrow Ar + (N_2^{2+})^* \rightarrow Ar + N^+ + N^+. \qquad (4)$$

in which nitrogen "seizes" all the charge from doubly charged Ar^{2+} ions, which are produced in e-beam-excited argon in a noticeable amount (Langhoff, 1994). Such ions finally convert into Ar_2^+ and Ar^+ ions (Wieser *et al.*, 2000) with the latter, in turn, converting into Ar_2^+ ions. The rate of the energy transfer to nitrogen seems to be high enough for nitrogen added in amount of about 3% apparently depletes high-lying energy reservoir ($Ar^{2+}(^3P)$ in (4)) as further increase in nitrogen pressure causes only slight effect. Contrary to the case of Ar/N_2 mixture, reaction of less energetic Kr^{2+} ions with nitrogen is known to proceed exclusively *via* single charge (electron) transfer (Smith *et al.*, 1980)

$$Kr^{2+}(^3P) + N_2 \rightarrow Kr^+ + N_2^+, \qquad (5)$$

and thus does not lead to equally drastic reduction in Kr_2^+ number density; however, it should be somewhat decreased. Nitrogen is known to reduce the intensity of the second emission continuum (145 nm) related to Kr_2^* (Kanaev *et al.*, 1993): then, one could have supposed that the long-wavelength fraction of the absorption continuum decreasing with nitrogen was related to Kr_2^*. However, in Ne/Kr mixtures, there is no continuous absorption at all whereas absorption related to Kr*(5*s*) is definitely present (see Fig. 4a and Levchenko *et al.* (2010*a*)). Absolute concentration of Kr is not small, and as long as there are Kr*(5*s*) atoms, there also have to be Kr_2^* dimers responsible for the emission in the second continuum. Hence, whole 320-nm absorption continuum is caused by only Kr_2^+; its absorption maximum and long-wavelength fraction are related, respectively, to low-*v* and high-*v* states of Kr_2^+ (see Levchenko *et al.* (2010*a*)) with the latter being collisionally quenched by N_2. Such collisional quenching enlarges population of low-*v* levels and increases 320-nm absorption, which might compensate the reduction in the production rate of Kr_2^+ due to reaction (5). As a result, there is no noticeable decrease in the maximum of continuum absorption with adding nitrogen to Kr. Similarly, observed reduction in the absorption at $\lambda \sim 460$ nm in $Ar/Kr/F_2/N_2$ mixture can be caused by enhanced vibrational relaxation of Kr_2F ($4^2\Gamma$, $v >> 0$). In the light of above, one can expect that, after adding nitrogen to Kr/F_2 mixture, spurious transfer of energy to nitrogen reducing excitation rate will be minimal whereas collisional quenching of vibrationally excited Kr_2F is to proceed.

4. CONCLUSION

Transient absorption has been measured with the novel erosion-plasma-source probe technique in a broad spectral range 190–510 nm for Ar(He, Ne)/Kr/NF_3($F_2 + N_2$) gas mixtures under e-beam excitation rate of 1 MW/cm^3 typical of rare-gas halide laser operation. It is experimentally observed that, in Kr/F_2 and Ar/F_2 mixtures, fluorescence and absorption spectra of Rg_2F species are shifted with respect to each other in the opposite direction. Continuous absorption spectrum of Ar_2F excimer is reported, as far as we know, for the first time in the refereed literature. Strong overlapping between the fluorescence and absorption spectra of Ar_2F is responsible for the absence of lasing on Ar_2F molecule. Absorption spectrum of Kr_2F excimer is recorded in pure form using a $Ne/Kr/F_2$ mixture with no alternative broadband absorber. It is found that minor additive of nitrogen to $Ar/Kr/F_2$ mixture or use of NF_3 instead of F_2 reduces transient absorption in the blue range and results in broadband optical amplification centered at about 460 nm. Both amplification by nitrogen-containing species (e.g., N_2KrF^*) and nitrogen-caused enhancement of vibrational relaxation in Kr_2F ($4^2\Gamma$), reducing population of the absorbing states, can be the reason. The maximum amplification is estimated as $\sim 0.1 \pm 0.05$ m^{-1}. Further experiments with improved accuracy were performed in seven-pass scheme with Ar/Kr/NF_3 mixture using a 25-ns-long (FWHM) narrow-band probe pulse of dye laser at $\lambda \sim 460$ nm (Levchenko *et al.*, 2010*c*). By varying the time delay of the probe pulse with respect to the beginning of e-beam pumping, it was demonstrated that maximum gain of 0.1 m^{-1} occurs at time delay about 100 ns, which corresponds to maximum fluorescence of Kr_2F. Such gain is high enough to amplify femtosecond laser pulses in a muti-pass amplifier layout.

ACKNOWLEDGMENTS

The study was supported by the U.S. Naval Research Laboratory; Russian Foundation for Basic Research, project no. 08-02-01331; fundamental research programs of Presidium RAS "Problems of physical electronics of charged particle beams and generation of electromagnetic radiation in high-power systems" and "Extremal light fields and their applications."

REFERENCES

Basov, N.G., Gus'kov, S.Yu. & Feoktistov, L.P. (1992). Thermonuclear gain of ICF targets with direct heating of ignitor. *J. Sov. Laser Res.* **13**, 396–399.

Basov, N.G., Zuev, V.S., Kanaev, A.V., Mikheev, L.D. & Stavrovskii, D.B. (1980). Stimulated emission from the triatomic excimer Kr_2F subjected to optical pumping. *Sov. J. Quant. Electron.* **7**, 2660–2661.

Betti, R, Zhou, C.D., Anderson, K.S., Perkins, L.J., Theobald, W. & Solodov, A.A. (2007). Shock ignition of thermonuclear fuel with high areal density. *Phys. Rev. Lett.* **98**, 155001-1/155001-4.

Bigio, I.J., Czuchlewski, S.J., Mccown, A.W. & Taylor, A.J. (1990). Recent Advances in Excimer Laser Technology at Los Alamos. *Los Alamos Unclassified Report* LAUR-89-2875, http://catalog.lanl.gov/F.

Boichenko, A.M., Tarasenko, V.F. & Yakovlenko, S.I. (2000). Exciplex Rare–Halide Lasers. *Laser Physics* **10**, 1159–1187.

Brau, C.A. (1984). Rare gas Halogen excimers. In *Topics in Applied Physics* (Rhodes Ch.K., Ed.), Vol. 30, pp. 87–138. New York: Springer.

Chantry, P.J. (1982). Negative ion formation in gas lasers. In *Applied Atomic Collision Physics* (McDaniel E.W. & Nighan W.L., Eds), Vol 3, Chapter 2. New York: Academic Press.

Ernst, W.E.,Tittel, F.K., Wilson, W.L. & Marowsky, G. (1979). Gain conditions for electron-beam-excited Ar-N_2 laser lines at 337.1, 357.7, and 380.5 nm. *J. Appl. Phys.* **50**, 3879–3883.

Geohegan, D.B. & Eden, J.G. (1988). Absorption spectrum of $Kr_2F(4\,^2\Gamma)$ in the near ultraviolet and visible ($335 \leq \lambda \leq 600$ nm): Comparison with $Kr_2^+(1(1/2)_u)$ measurements. *J. Chem. Phys.* **89**, 3410–3427.

Greene, D.P. & McCown, A.W. (1989). Transient absorpion spectrosopy of $Kr_2F(4^2\Gamma)$. *Appl. Phys. Lett.* **54**, 1965–1967.

Huestis, D.L., Marowsky, G. & Tittel, F.K. (1984). Triatomic rare-gas-Halide excimers. In *Topics in Applied Physics* (Rhodes Ch.K., Ed.), Vol. 30, pp. 181–216. New York: Springer.

Kanaev, A.V., Zafiropulos, V., Ait-Kaci, M., Museur, L., Nkwawo, H. & Castex, M.C. (1993). Excimer formation mechanism in gaseous krypton and Kr/N_2 mixtures. *J. Phys. D* **27**, 29–37.

Langhoff, H. (1994). The origin of the higher continua emitted by the rare gases. *J. Phys. B: At. Mol. Opt. Phys.* **27**, L709–L714.

Levchenko, A.O., Ustinovskii, N.N. & Zvorykin, V.D. (2010*a*). Absorption spectra of e-beam-excited Ne, Ar and Kr, pure and in binary mixtures. *J. Chem. Phys.* **133**, 154301/154310.

Levchenko, A.O., Ustinovskii, N.N. & Zvorykin, V.D. (2010*b*). Novel technique for transient absorption probing. *J. Russian Laser Res.* **31**, 475–480.

Levchenko, A.O., Zvorykin, V.D., Likhomanova, S.V., Ustinovskii, N.N. & Shtan'ko, V.F. (2010*c*). Amplification and generation of radiation at the $4^2\Gamma \rightarrow 1,2^2\Gamma$ transition of the Kr_2F molecule in an electron-beam-pumped wide-aperture laser. Q*uan. Electr.* **40**, 203–209.

Mandl, A. & Hyman, H.A. (1986). N_2 excited state absorption in XeF laser. *Appl. Phys. Lett.* **49**, 841–843.

Marowsky, G., Glass, G.P., Tittel, F.K., Hohla, K., Wilson Jr., W.L. & Weber, H. (1982). Formation kinetics of the triatomic excimer Ar_2F. *IEEE J. QE.* **18**, 898–902.

McCown, A.W., Ediger, M.N., Geohegan, D.B. & Eden, J.G. (1985). Absorption of electronically excited Xe_2Cl in the ultraviolet. *J. Chem. Phys.* **82**, 4862–4866.

Miller, M., Friedman, J.F., Miller, A.E.S. & Paulson, J.F. (1995). Thermal electron attachment to NF_3, PF_3, and PF_5. *Internat. J. Mass Spectr. Ion Proc.* **149–150**, 111–121.

Molchanov, A.G. (1988). Theory of active media of excimer lasers. *Proc. of Lebedev Phys. Inst.* **171**, 72–167.

Molchanov, A.G. (2006). Short pulse amplification in a KrF-laser and the petawatt excimer laser problem. *J. Phys. IV France* **133**, 665–668.

Obenschain, S.P., Sethian, J.D. & Schmitt, A.J. (2009). A laser based fusion test facility. *Fusion Sci. Techn.* **56**, 594–603.

Pressley, R.J. (1971). *Handbook of Lasers with Selected Data on Optical Technology*. Cleveland: Chemical Rubber Co.

Rokni, M. & Jacob, J.H. (1982). Rare-gas Halide lasers. In *Applied Atomic Collision Physics* (McDaniel E.W. & Nighan W.L., Eds.), Vol. 3, Chapter 10. New York: Academic Press.

Sauerbrey, R., Tittel, F.K., Wilson Jr., W.L. & Nighan, W.L. (1982). Effect of nitrogen on XeF(C-A) and Xe_2Cl laser performance. *IEEE J.QE.* **18**, 1336–1340.

Sauerbrey, R., Zhu, Y., Tittel, F.K. & Wilson Jr., W.L. (1986). Optical emission and kinetic reactions of a four-atomic rare gas halide exciplex: Ar_3F. *J. Chem. Phys.* **85**, 1299–1302.

Schloss, J.H., Tran, H.C. & Eden, J.G. (1997). Photo dissociation of $Kr_2F(4\,^2\Gamma)$ in the ultraviolet and near-infrared: Wavelength dependence of KrF ($B\,^2\Sigma$) yield. *J. Chem. Phys.* **106**, 5423–5428.

Shannon, D.C., Killeen, K.P. & Eden, J.G. (1988). Br_2 ion pair state formation by electron beam excitation. *J. Chem. Phys.* **88**, 1719–1731.

Shaw, M.J. & Jones, J.D.C. (1977). Measurements of some reaction rates of importance in KrF lasers. *Appl. Phys.* **14**, 393–398.

Sherbakov, V.A. (1983). Calculation of thermonuclear laser target ignition by focusing shock wave. *Sov. J. Plasma Phys.* **9**, 240–244.

Smith, D., Adams, N.G., Alge, E., Villinger, H. & Lindinger, W. (1980). Reactions of Ne^{2+}, Ar^{2+}, Kr^{2+} and Xe^{2+} with the rare gases at low energies. *J. Phys. B: Atom. Mol. Phys.* **13**, 2787–2799.

Tabak, M., Hammer, J., Glinsky, M.E., Kruer, W.L., Wilks, S.C., Woodworth, J., Campbell, E.M. & Perry, M.D. (1994). Ignition and high gain with ultrapowerful lasers. *Phys. Plasmas* **1**, 1626–1634.

TELLINGHUISEN, J. (1982). Spectroscopy and excited state chemistry of excimer lasers. In *Applied Atomic Collision Physics* (McDaniel E.W. & Nighan W.L., Eds), Vol. 3. Chapter 9. New York: Academic Press.

TITTEL, F.K., SMAYLING, M. & WILSON, W.L. (1980). Blue laser action by rare-gas halide trimer Kr_2F. *Appl. Phys. Lett.* **37**, 862–864.

WADT, W.R. & HAY, P.J. (1978). Electronic states of Ar_2F and Kr_2F. *J. Chem. Phys.* **68**, 3850–3863.

WADT, W.R. (1980). The electronic states of Ne_2^+, Ar_2^+, Kr_2^+, and Xe_2^+. II. Absorption cross sections for the $1(1/2)_u \rightarrow 1(3/2)_g$, $1(1/2)_g$, $2(1/2)_g$ transitions. *J. Chem. Phys.* **73**, 3915–3926.

WIESER, J., ULRICH, A., FEDENEV, A. & SALVERMOSER, M. (2000). Novel pathways to the assignment of the third rare gas excimer continua. *Opt. Comm.* **173**, 233–245.

XU, J., GADOMSKI, W. & SETSER, D.W. (1993). Electronic quenching rate constants of KrF(*B,C*) and Kr_2F^*. *J. Chem. Phys.* **99**, 2591–2600.

ZUEV, V.S., KANAEV, A.V., MIKHEEV, L.D. & STAVROVSKII, D.B. (1981). Investigation of luminescence in the 420 nm range as a result of photolysis of KrF_2 in mixtures with Ar, Kr, and N_2. *Sov. J. Quant. Electron.* **11**, 1330–1335.

ZVORYKIN, V.D., ARLANTSEV, S.V., BAKAEV, V.G., RANTSEV, O.V., SERGEEV, P.B., SYCHUGOV, G.V. & TSERKOVNIKOV, A.Y. (2001). Transport of electron beams and stability of optical windows in high-power e-beam-pumped krypton fluoride lasers. *Laser Part. Beams* **19**, 609–622.

ZVORYKIN, V.D., DIDENKO, N.V., IONIN, A.A., KHOLIN, I.V., KONYASHCHENKO, A.V., KROKHIN, O.N., LEVCHENKO, A.O., MAVRITSKII, A.O., MESYATS, G.A., MOLCHANOV, A.G., ROGULEV, M.A., SELEZNEV, L.V., SINITSYN, D.V., TENYAKOV, S.YU., USTINOVSKII, N.N. & ZAYARNYI, D.A. (2007). GARPUN-MTW: A hybrid Ti:-Sapphire/KrF laser facility for simultaneous amplification of subpicosecond/nanosecond pulses relevant to fast-ignition ICF concept. *Laser Part. Beams* **25**, 435–451.